

Rational Design of Highly Active “Hybrid” Phosphine–Phosphinite Pincer Iridium Catalysts for Alkane Metathesis

Agnieszka J. Nawara-Hultzsch,[†] Jason D. Hackenberg,[†] Benudhar Punji,[†] Carolyn Supplee,^{†,‡} Thomas J. Emge,[†] Brad C. Bailey,[‡] Richard R. Schrock,[‡] Maurice Brookhart,[§] and Alan S. Goldman^{*,†}

[†]Department of Chemistry and Chemical Biology, Rutgers, The State University of New Jersey, New Brunswick, New Jersey 08903, United States

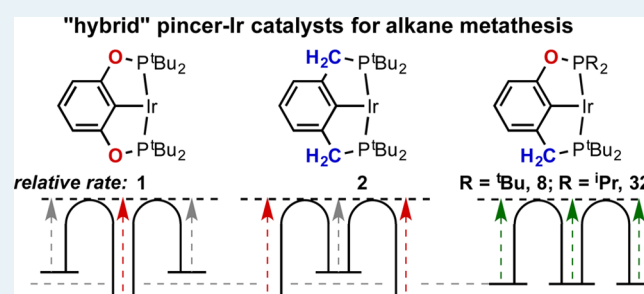
[‡]Department of Chemistry, Massachusetts Institute of Technology, Cambridge, Massachusetts 02139, United States

[§]Department of Chemistry, The University of North Carolina at Chapel Hill, Chapel Hill, North Carolina 27599, United States

S Supporting Information

ABSTRACT: Both the bisphosphine and bisphosphinite pincer complexes ($i^{\text{Bu}}_4\text{PCP}$)IrH₂ and ($i^{\text{Bu}}_4\text{POCOP}$)IrH₂ can cocatalyze alkane metathesis in tandem with olefin metathesis catalysts, but the two complexes have different resting states during catalysis, suggesting that different steps are turnover-limiting in each case. This led to the hypothesis that a complex with intermediate properties would be catalytically more active than either of these two species. Accordingly, “hybrid” phosphine–phosphinite pincer ligands (PCOP) and the corresponding iridium complexes were synthesized (3c–e). In tandem with olefin-metathesis catalyst MoF12, ($i^{\text{Bu}}_4\text{PCOP}$)IrH₂ displays significantly higher activity for the metathesis of *n*-hexane than does ($i^{\text{Bu}}_4\text{PCP}$)IrH₂ or ($i^{\text{Bu}}_4\text{POCOP}$)IrH₂. ($i^{\text{Bu}}_2\text{PCOP}^{\text{Ir}2}$)IrH₄ (3d) is even more active (>30-fold more active than ($i^{\text{Bu}}_4\text{POCOP}$)IrH₂) and affords nearly 4.6 M alkane products after 8 h at 125 °C.

KEYWORDS: pincer complexes, alkane metathesis, homogeneous catalysis, dehydrogenation, iridium



INTRODUCTION

The gap between global consumption of liquid fuels and production of conventional crude oil is expected to widen dramatically over the next several decades.^{1–4} Although conventional crude is the source of >90% of liquid fuel consumed today, Brandt et al. have estimated that fraction will decline to roughly 50% by 2050 and perhaps 15% by 2080,¹ although the rate of this change has a high degree of uncertainty, the direction and the eventual magnitude does not. The gap will be met by large increases in the use of “natural gas liquids” and condensates (low-molecular-weight hydrocarbons from geologic sources) and, especially, “unconventional liquids” of origin that is yet to be determined.^{1,4} Fischer–Tropsch (F–T) catalysis is likely to play an important role in the context of unconventional liquid fuel production.^{5–7} The feedstock for F–T may be derived from coal or natural gas (the current sources for commercial reactors), from biomass,^{8–12} or from CO₂/H₂O with energy input from carbon-free sources.^{13–16}

The increased demand for liquid fuel is driven specifically by increased demand for diesel and jet fuel,^{4,17} both of which are generally of high molecular weight (typically ca. C₉–C₁₉ and C₈–C₁₆, respectively). Although F–T catalysis followed by hydrocracking of the heavier products can give high yields in this range, lighter *n*-alkanes are still produced in substantial

amounts. Further, natural gas liquids and condensates are composed exclusively of alkanes with molecular weights well below this desirable range. Thus, we can anticipate a critical need for the development of practical methods for the large-scale catalytic conversion of light alkanes to heavier-molecular-weight species.

The only general method reported to date for the direct conversion of light alkanes to heavier alkanes is alkane metathesis. Alkane metathesis with heterogeneous catalysts has been reported by Burnett and Hughes¹⁸ and by Basset and Coperet et al.¹⁹ These systems represent major breakthroughs, but they suffer from limitations, including the need for severe reaction conditions, relatively low reaction rates, and low selectivity with respect to the formation of higher molecular weight and unbranched species.

We have previously reported the catalytic metathesis of *n*-alkanes based on a tandem process that utilizes an iridium-based catalyst for alkane dehydrogenation and an olefin metathesis catalyst to metathesize the alkenes generated in situ (Figure 1).^{20–22} The hydrogen removed from the alkanes is then used to hydrogenate the metathesized olefin products.

Received: July 30, 2013

Revised: September 19, 2013

Published: September 23, 2013

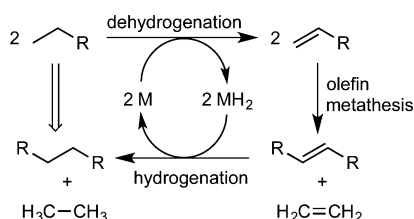


Figure 1. Alkane metathesis via tandem dehydrogenation–hydrogenation and olefin metathesis catalysis.

Since the olefin metathesis catalysts afford high reaction rates even at ambient temperatures, whereas alkane metathesis and simple transfer–dehydrogenation require temperatures >100 °C to achieve even modest rates, it is presumed that the transfer–dehydrogenation component limits the rate of alkane metathesis; however, it is not obvious which segment of the transfer–dehydrogenation cycle (hydrogenation or dehydrogenation) is rate-limiting.

In the case of dehydrogenation at the alkane terminus and metathesis of the resulting α -olefins, the product of metathesis of n -alkane C_nH_{2n+2} is $C_{2n-2}H_{4n-2}$ plus ethane, as illustrated in Figure 1.^{20,21}

Our previous reports have focused on PCP- and POCOP-ligated iridium catalysts (Figure 2) for dehydrogenation^{20,21} in

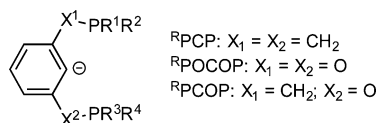


Figure 2. Pincer ligands of the type used in this work ($X = CH_2$ or O ; $R = \text{alkyl}$).

combination with various types of olefin metathesis catalysts, including molecular species,²³ such as $\text{Mo}(\text{NAr})(\text{CHCMe}_2\text{Ph})[\text{OCMe}(\text{CF}_3)_2]_2$ ($\text{Ar} = 2,6\text{-iPrC}_6\text{H}_3$) (**MoF12**), as well as traditional heterogeneous olefin metathesis catalysts, such as Re_2O_7 on γ -alumina.²⁴

In our initial work, we observed that similar rates of alkane metathesis were obtained with PCP ($X^1, X^2 = CH_2$) and POCOP ($X^1, X^2 = O$) iridium species (operating in tandem with **MoF12**).^{19,20} We therefore focused, in our initial attempts to improve rates, on varying the phosphinoalkyl groups, the nature of which presumably dominated steric effects; this approach has, indeed, yielded faster catalytic systems.^{23–25} Herein, however, we report that mechanistic considerations have led us to consider variation of the linker groups X , in

particular, “hybrid” or “PCOP” pincer catalysts in which $X^1 = CH_2$, and $X^2 = O$). These hybrid PCOP complexes are, indeed, found to be highly effective, yielding the highest catalytic activities reported to date for this class of alkane metathesis catalysts.

RESULTS AND DISCUSSION

The pincer ligands that have been most commonly used for alkane metathesis and alkane dehydrogenation more generally²⁶ are ${}^t\text{Bu}^4\text{PCP}$ ($R^1, R^2, R^3, R^4 = {}^t\text{Bu}$; $X^1, X^2 = CH_2$; **1a**) and ${}^t\text{Bu}^4\text{POCOP}$ ($R^1, R^2, R^3, R^4 = {}^t\text{Bu}$; $X^1, X^2 = O$; **1b**). At the outset of our studies, we found that complexes of these ligands afforded relatively similar rates of alkane metathesis. This similarity notwithstanding, the resting states of the complexes were quite different. Specifically, the resting states were found to be $({}^t\text{Bu}^4\text{PCP})\text{IrH}_2$ and $({}^t\text{Bu}^4\text{POCOP})\text{Ir}(\text{olefin})$, respectively, with no evidence of the “converse” species, $({}^t\text{Bu}^4\text{PCP})\text{Ir}(\text{olefin})$ and $({}^t\text{Bu}^4\text{POCOP})\text{IrH}_2$, detected under catalytic conditions in situ.

It might be presumed that catalytic transfer–dehydrogenation by ${}^t\text{Bu}^4\text{PCP}$ and ${}^t\text{Bu}^4\text{POCOP}$ catalysts proceeds by analogous pathways, and indeed, there is a considerable body of evidence that supports this presumption.^{27–30} The observed difference in resting states therefore implies that although the pathways may be analogous, the respective rate-determining steps in the catalytic cycles are different for the two catalysts. Specifically, the $({}^t\text{Bu}^4\text{PCP})\text{IrH}_2$ resting state implies that olefin hydrogenation is rate-determining, whereas the $({}^t\text{Bu}^4\text{POCOP})\text{Ir}(\text{olefin})$ resting state implies that the rate-determining step involves loss of olefin (possibly reversible), followed by alkane dehydrogenation. Moreover, this suggests that the corresponding step for each catalyst that is *not* rate-determining is relatively fast; for example, olefin hydrogenation by $({}^t\text{Bu}^4\text{POCOP})\text{IrH}_2$.³¹ Thus, for the ${}^t\text{Bu}^4\text{PCP}$ catalyst, the alkane-hydrogenation segment of the cycle is relatively slow, and the alkane-dehydrogenation segment (including dissociation of olefin to give the active fragment, (pincer) Ir ³²) is relatively fast, whereas the converse is true for the ${}^t\text{Bu}^4\text{POCOP}$ catalyst.

We considered the possibility that if the catalytic cycles of the ${}^t\text{Bu}^4\text{PCP}$ and ${}^t\text{Bu}^4\text{POCOP}$ catalysts include converse sets of one slow and one fast segment, then the catalytic cycle of a species whose properties are intermediate between ${}^t\text{Bu}^4\text{PCP}$ and ${}^t\text{Bu}^4\text{POCOP}$ could contain two segments with rates that are each intermediate between the two extremes. If, indeed, the two segments have intermediate rates, rather than one fast and one slow, the overall catalytic rate of such a species would be faster

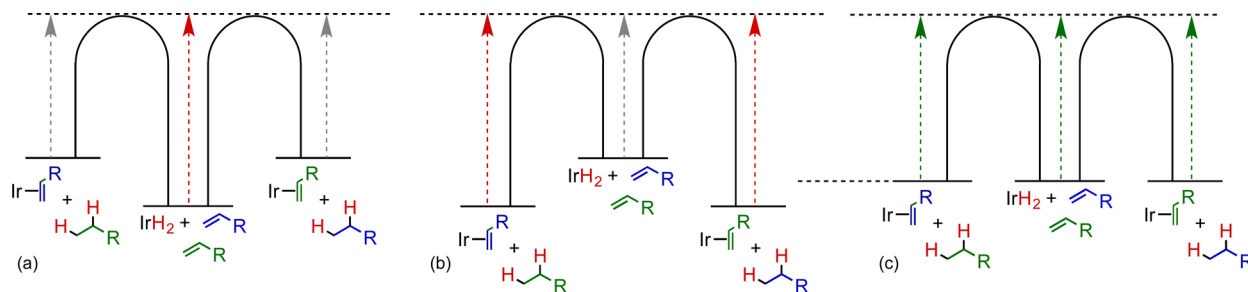
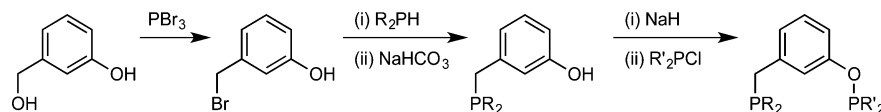
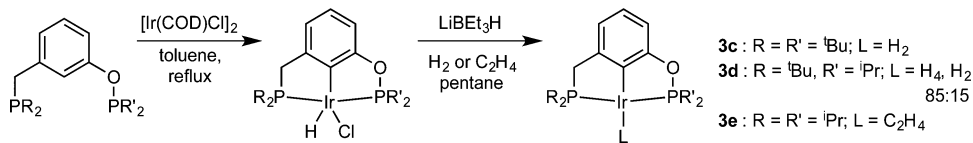


Figure 3. Schematic diagram indicating relative overall free energy barriers, under alkane metathesis conditions, for the alkane dehydrogenation and olefin hydrogenation segments of the transfer–dehydrogenation catalytic cycle for (a) $({}^t\text{Bu}^4\text{PCP})\text{Ir}$, (b) $({}^t\text{Bu}^4\text{POCOP})\text{Ir}$, and (c) a hypothetical species with properties intermediate between $({}^t\text{Bu}^4\text{PCP})\text{Ir}$ and $({}^t\text{Bu}^4\text{POCOP})\text{Ir}$.

Scheme 1. Synthesis of “PCOP-H” Ligand Precursors



Scheme 2. Metalation of PCOP-H Ligand Precursors To Form (PCOP)IrHCl and Subsequent Reduction to Catalyst Precursors



than that of either ^{*t*Bu}PCP or ^{*t*Bu}POCOP catalysts. This is illustrated, in a completely schematic fashion, with the free energy diagram in Figure 3.

The most obvious candidate for a species with properties (including reactivity) intermediate between that of (^{*t*Bu}PCP)Ir and (^{*t*Bu}POCOP)Ir catalysts would be a “hybrid” phosphine–phosphinite species (^{*t*Bu}PCOP)Ir (Figure 2; X₁ = CH₂, X₂ = O, R = *t*-Bu).

Synthesis and Characterization of PCOP Ligands and Iridium Complexes. The ^{*t*Bu}PCOP-H ligand precursor (**1c-H**) was prepared following the method used by Eberhard and Jensen³³ (Scheme 1) to synthesize ^{*t*Bu}PCOP^{*i*Pr}₂-H (Figure 2; X₁ = CH₂; X₂ = O; R₁, R₂ = *t*-Bu; R₃, R₄ = *i*-Pr). A pale yellow viscous oil was obtained in 84% yield. The ³¹P NMR spectrum displayed a peak at 152.7 ppm corresponding to the O–P^{*t*Bu}₂ moiety (cf. ^{*t*Bu}POCOP-H, δ 153.1 ppm) and a peak at 34.1 ppm corresponding to the CH₂–P^{*t*Bu}₂ moiety (cf. ^{*t*Bu}PCP-H, δ 33.0 ppm). The crude oil was used without further purification.

Metalation of the crude ligand precursor with [Ir(COD)Cl]₂ in refluxing toluene occurred cleanly to yield the corresponding (^{*t*Bu}PCOP)IrHCl species (**2c**) in 68% isolated yield as analytically pure, air-stable, red microcrystalline solids after recrystallization from pentane (Scheme 2). The ³¹P{¹H} NMR spectrum of **2c** displayed a doublet of doublets at 168.6 ppm (²J_{PP} = 345.0 Hz, ²J_{PH} = 12.3 Hz) attributable to the O–P^{*t*Bu}₂ group (cf. (^{*t*Bu}POCOP)IrHCl,³⁰ δ 175.8 ppm) and 70.6 ppm (²J_{PP} = 345.0 Hz, ²J_{PH} = 11.0 Hz) attributable to the CH₂–P^{*t*Bu}₂ group (cf. δ 67.3 ppm, ²J_{PH} = 12.4 Hz for (^{*t*Bu}PCP)IrHCl^{34,35}). The large value of ²J_{PP} (345.0 Hz) is characteristic of mutually trans-coordinated inequivalent ³¹P nuclei. In the ¹H NMR spectrum, the hydride is manifest with a doublet of doublets at δ –41.38 ppm (²J_{PH} = 13.3 Hz, ²J_{PH} = 12.3 Hz) that is nearly identical to the corresponding shifts of the nonhybrid species and is attributable to an apical hydride trans to a vacant coordination site in a 5-coordinate square pyramidal (pincer)Ir complex.^{30,35}

Compound **2c** was further characterized by X-ray crystallography (Figure 4). The coordination geometry is approximately square pyramidal with the hydride located in the apical position. Selected bond lengths and angles are summarized in Table 1. The Ir–P(O) bond length is 2.269 Å, slightly shorter than the Ir–P bond lengths 2.295(±2) in (^{*t*Bu}POCOP)IrHCl. The Ir–P(CH₂) bond length is 2.319 Å, slightly longer than that reported³⁶ for (^{*t*Bu}PCP)IrHCl (2.305(±1) Å). These values all seem consistent with a greater trans influence exerted by the phosphinite vs the phosphine groups.

The P(1)–Ir–P(2) bond angle of **2c** (163.6°) is slightly less than that of (^{*t*Bu}PCP)IrHCl³⁴ (**2a**, 164.3°)³⁶ and greater than

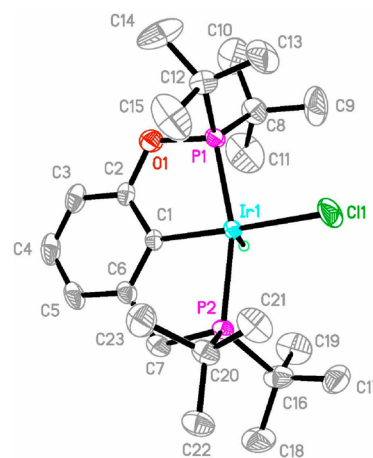


Figure 4. Thermal ellipsoid plot of (^{*t*Bu}PCOP)IrHCl (**2c**). Hydrogen atoms other than the hydride ligand omitted for clarity.

Table 1. Selected Bond Distances (Å) and Bond Angles (°) for (^{*t*Bu}PCOP)IrHCl (**2c**)

bond distances (Å)		bond angles (deg)	
Ir(1)–C(1)	2.016(3)	C(1)–Ir(1)–P(1)	81.27(10)
Ir(1)–P(1)	2.2685(9)	C(1)–Ir(1)–P(2)	82.47(10)
Ir(1)–P(2)	2.3194(8)	P(1)–Ir(1)–P(2)	163.55(3)
Ir(1)–Cl(1)	2.4012(10)	C(1)–Ir(1)–Cl(1)	177.71(9)
P(1)–O(1)	1.662(3)	P(1)–Ir(1)–Cl(1)	97.03(3)
P(1)–C(8)	1.848(4)	P(2)–Ir(1)–Cl(1)	99.16(3)
P(1)–C(12)	1.852(4)	O(1)–P(1)–C(8)	101.01(18)
P(2)–C(7)	1.814(4)	O(1)–P(1)–Ir(1)	104.63(10)
P(2)–C(16)	1.868(4)	C(7)–P(2)–Ir(1)	102.67(13)
P(2)–C(20)	1.865(4)	C(2)–O(1)–P(1)	115.2(2)
		C(6)–C(7)–P(2)	111.0(3)

that of (^{*t*Bu}POCOP)IrHCl (**2b**, 160.1°).³⁷ The C–Ir–P(CH₂) bond angles (82.5°) are similar to those reported for **2a** (82.0°, 82.3°), and the C–Ir–P(O) angle (81.3°) is slightly greater than the corresponding angles in (^{*t*Bu}POCOP)IrHCl (80.0°, 80.1°).³⁰

A solution of **2c** was treated with LiEt₃BH under H₂ atmosphere, resulting in 93% conversion to (^{*t*Bu}PCOP)IrH₂ (**3c**). Complex **3c** displayed ³¹P{¹H} NMR signals consistent with those of its symmetrical analogues, exhibiting a doublet at δ 200.3 ppm (²J_{PP} = 330 Hz) attributable to the O–P(*t*Bu)₂ group (cf. (^{*t*Bu}PCOP)IrH₂, δ 204.9 ppm) and a doublet at 87.3 ppm (²J_{PP} = 330 Hz) due to the CH₂–P(*t*Bu)₂ group (cf. (^{*t*Bu}PCP)IrH₂, δ 86.1 ppm). The hydride signal in the ¹H NMR spectrum appeared as a triplet at δ –18.12 ppm with ²J_{PH}

Table 2. Product Concentrations (mM) of Products Formed by Metathesis of *n*-Hexane (7.5 M) Catalyzed by MoF12 (16 mM) and Catalysts 3a, 3b, 3c (10 mM) at 125 °C

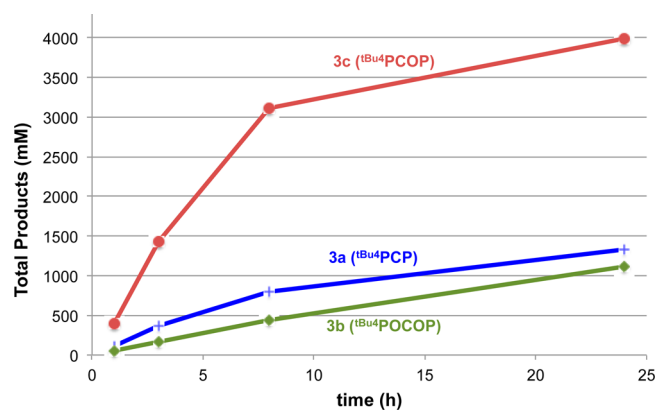
Catalyst 3b, (^t Bu ² POCOP ^t Bu ²)IrH ₂												
<i>t</i> (h)	C2	C3	C4	C5	C7	C8	C9	<i>trans</i> -5-decene	C10	C11–19	[total product]	selectivity C10/(C7–10)
1	2	12	11	10	7	4	3	2	2	1	54	0.22
3	4	38	34	34	22	14	9	2	6	7	171	0.15
8	7	93	81	94	64	40	28	1	19	14	442	0.13
24	15	232	194	249	168	98	76	1	47	33	1111	0.12
Catalyst 3a, (^t Bu ² PCP ^t Bu ²)IrH ₂												
<i>t</i> (h)	C2	C3	C4	C5	C7	C8	C9	<i>trans</i> -5-decene	C10	C11–19	[total product]	selectivity C10/(C7–10)
1	21	14	21	22	11	1	4	11	7	0	113	0.55
3	63	52	30	100	57	6	10	14	38	1	370	0.42
8	165	96	62	200	121	14	19	12	106	10	805	0.43
24	295	158	119	303	167	26	32	7	202	25	1335	0.48
Catalyst 3c, (^t Bu ² PCOP ^t Bu ²)IrH ₂												
<i>t</i> (h)	C2	C3	C4	C5	C7	C8	C9	<i>trans</i> -5-decene	C10	C11–19	[total product]	selectivity C10/(C7–10)
1	12	82	53	103	67	28	20	2	19	15	401	0.16
3	33	317	215	339	233	115	74	2	55	53	1437	0.12
8	85	708	495	727	477	234	145	2	104	134	3111	0.11
24	156	896	639	948	576	267	183	2	162	168	3997	0.14

= 8.6 Hz. Comparison with the corresponding values for the symmetrical analogues supports the assumption that 3c should have properties intermediate between (^tBu⁴POCOP)IrH₂ (δ -17.4 ppm, $^2J_{\text{PH}} = 8.2$ Hz) and (^tBu⁴PCP)IrH₂ (δ -19.2 ppm, $^2J_{\text{PH}} = 8.8$ Hz).

Catalytic Activity of (^tBu⁴PCP)Ir, (^tBu⁴POCOP)Ir and (^tBu⁴PCOP)Ir for Alkane Metathesis. Alkane metathesis reactions catalyzed by (^tBu⁴PCOP)IrH₂ (3c) as well as the previously reported symmetrical complexes (^tBu⁴POCOP)IrH₂ (3b) and (^tBu⁴PCP)IrH₂ (3a) were performed with 10 mM of the (pincer)Ir catalyst, 16 mM of the olefin metathesis catalyst, Mo(NAr)(CHCMe₂Ph)[OCMe(CF₃)₂] (Ar = 2,6-*i*-PrC₆H₃) (MoF12), 30.0 mM mesitylene (internal GC standard), and *n*-hexane as the solvent/substrate (~7.6 M). 3,3-Dimethyl-1-butene (TBE; 20 mM) was added as a hydrogen acceptor to dehydrogenate the active catalyst and to generate a steady-state concentration of olefin (see Figure 1).

All experiments were performed under an argon atmosphere. Reactions were conducted at 125 °C in flame-sealed tubes, and the progress of the reaction was monitored by gas chromatography at intervals of 1, 3, 8, and 24 h, with three tubes opened at each time. Reported values represent the average of the three runs.

Complex 3c is found to be a remarkably active catalyst (Table 2 and Figure 5), strongly supporting the hypothesis that a “hybrid” species with properties intermediate between those of (^tBu⁴POCOP)Ir and (^tBu⁴PCP)Ir would display activity greater than that of either of the symmetrical complexes. For the first 8 h, all three catalysts display roughly constant turnover frequencies. The relative conversions for (^tBu⁴POCOP)Ir, (^tBu⁴PCP)Ir, and (^tBu⁴PCOP)Ir are approximately (1 h: 1:2.1:7.4), (3 h: 1:2.2:8.4), and (8 h: 1:1.8:7.0). Since a larger fraction of the hexane has undergone conversion in the (^tBu⁴PCOP)Ir-catalyzed reactions (e.g., 41% after 8 h), the values indicated for this catalyst are somewhat lower than the actual relative rates because of increased back-reactions that produce hexane as well as the decreased rate of reaction with hexane due to its lowered concentration.

**Figure 5.** Total alkane products formed in the metathesis of *n*-hexane catalyzed by MoF12 and catalysts 3a–c.

After 8 h, the reaction rates decrease. This presumably reflects decomposition of the MoF12 catalyst,^{20,23,38,39} decreased concentration of hexane (particularly in the case of catalyst 3c), and possibly some decomposition of (pincer)Ir. The concentration of total products obtained with 3c at 24 h is 4.0 M (52% conversion).

Our initial hypothesis was based on the premise that the transfer dehydrogenation cycles of (^tBu⁴PCP)Ir and (^tBu⁴POCOP)Ir each had one fast segment and one slow segment (for (^tBu⁴PCP)Ir alkane dehydrogenation is fast and olefin hydrogenation is slow, but the reverse is true for (^tBu⁴POCOP)Ir); a hybrid species would approach a limit whereby the rates of the two segments would be intermediate between the two extremes and the overall rate would therefore be greater.

To test the validity of this reasoning, we investigated the nature of the resting state in the (^tBu⁴PCOP)Ir-catalyzed reaction. An *n*-hexane solution of (^tBu⁴PCOP)IrH₂ (10 mM), MoF12 (16 mM), and TBE (40 mM) was prepared and monitored by ³¹P NMR at 90 °C. After 60 min, it exhibited two major sets of signals: a smaller set attributable to (^tBu⁴PCOP)IrH₂ and a larger set (a doublet at δ 171.2 ppm and doublet at δ

67.6 ppm) that appeared to be attributable to the olefin-bound complex. In a separate NMR tube, 40 mM 1-hexene was added to a *p*-xylene-*d*₁₀ solution of 10 mM ^tBu⁴PCOPIrH₂; this yielded the doublets at 171.2 and 67.6 ppm in the ³¹P NMR spectrum, indicating that the larger set of peaks is, indeed, attributable to an olefin-bound species. Thus, the mixture of hydride and olefin complex in the alkane solutions confirms that the rates of alkane dehydrogenation and olefin hydrogenation are, indeed, comparable with this catalyst.

Other PCOP-Based Complexes. Encouraged by our success with (^tBu⁴PCOP)Ir, we investigated the effect of varying the alkyl groups while maintaining the PCOP motif. We prepared, in analogy to the preparation of ^tBu⁴PCOP-H (Scheme 1), ⁱPr⁴PCOP-H and the previously reported³³ ^tBu²PCOPⁱPr²-H. The ³¹P NMR spectra of these PCOP ligand precursors were consistent with the spectra of the respective “non-hybrid” species, ^tBu⁴PCP, ^tBu⁴POCOP, ⁱPr⁴PCP, and ⁱPr⁴POCOP; that is, all signals in the ³¹P NMR spectra of the hybrids had chemical shifts similar to the ^tBu²PCH₂, ^tBu²PO, ⁱPr²PCH₂, and ⁱPr²PO groups in the respective symmetrical ligand precursors. The crude oils were used without further purification, and metalation with [Ir(COD)Cl]₂ yielded the corresponding (PCOP)IrHCl species in good yield (Scheme 2). Crystals of (^tBu²PCOPⁱPr²)IrHCl were obtained, and the molecular structure (Figure 6) was determined by X-ray

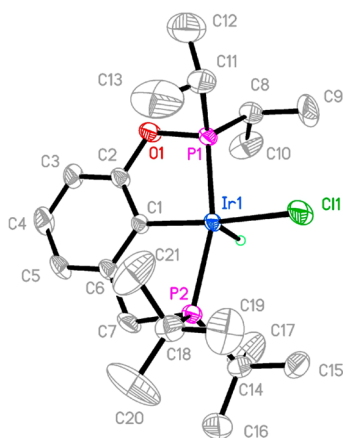


Figure 6. Thermal ellipsoid plot of (^tBu²PCOPⁱPr²)IrHCl (**2d**). Hydrogen atoms other than the hydride ligand omitted for clarity.

crystallography. Selected bond lengths and angles are summarized in Table 3. In general, the structure of **2d** is

Table 3. Selected Bond Lengths (Å) and Bond Angles (°) for (^tBu²PCOPⁱPr²)IrHCl (**2d**)

bond lengths (Å)		bond angles (deg)	
Ir(1)–C(1)	2.011(4)	C(1)–Ir(1)–P(1)	80.99(13)
Ir(1)–P(1)	2.2446(12)	C(1)–Ir(1)–P(2)	83.05(13)
Ir(1)–P(2)	2.3292(12)	P(1)–Ir(1)–P(2)	163.76(4)
Ir(1)–Cl(1)	2.3888(12)	C(1)–Ir(1)–Cl(1)	173.52(13)
P(1)–O(1)	1.643(4)	P(2)–Ir(1)–Cl(1)	97.03(3)
P(1)–C(8)	1.800(6)	P(1)–Ir(1)–Cl(1)	99.16(3)
P(1)–C(11)	1.848(7)	O(1)–P(1)–C(8)	101.9(3)
P(2)–C(7)	1.843(5)	O(1)–P(1)–Ir(1)	105.64(14)
P(2)–C(14)	1.866(5)	C(7)–P(2)–Ir(1)	102.59(18)
O(1)–C(2)	1.396(6)	C(2)–O(1)–P(1)	114.7(3)
		C(6)–C(7)–P(2)	110.6(3)

quite similar to that of **2c**. The Ir–P(O) distance is slightly shorter in **2d** (2.245 Å vs 2.269 Å in **2c**), presumably allowed by the less bulky *i*-Pr groups, whereas the Ir–P(CH₂) distance is slightly longer in **2d** (2.329 Å vs 2.319 Å), probably as a result of the greater trans influence due to the shorter Ir–P(O) distance. The P–Ir–P angle of **2d** is 163.76(4)°, nearly identical to that in **2c**, 163.55(3)°.

The hydride complex **3d** was prepared from (^tBu²PCOPⁱPr²)IrHCl (**2d**) in analogy with the synthesis of **3c**; this relatively uncrowded complex was isolated as an 85:15 mixture of the corresponding tetrahydride and dihydride. (Note that whereas (^tBu⁴PCP)IrH₄ easily loses H₂ to give the isolable (^tBu⁴PCP)IrH₂, the less crowded (ⁱPr⁴PCP)IrH₄ does not so readily lose H₂,⁴⁰ and the corresponding (ⁱPr⁴PCP)IrH₂ has not been reported.) Difficulty in synthesizing the analogous ⁱPr⁴PCOP iridium hydrides led us to conduct the reduction of **2e** with LiEt₃BH under ethylene atmosphere instead of dihydrogen, affording (ⁱPr⁴PCOP)Ir(C₂H₄) as a brown solid in 95% yield; (pincer)Ir olefin complexes are generally assumed to be functionally equivalent to the hydrides as catalyst precursors.²⁰

(^tBu²PCOPⁱPr²)IrH₄ (**3d**) afforded catalytic rates even greater than those of (^tBu⁴PCOP)IrH₂ (**3c**) (Table 4 and Figure 7). After 1 h (under the same conditions as the catalyzes discussed above), 1.75 M metathesis products were obtained, representing a rate 4.4 times that of **3c** or ~32 times that of (^tBu⁴POCOP)IrH₂ (**3b**). After 3 and 8 h, 3.2 and 4.6 M product was observed. **3d** is the most effective dehydrogenation catalyst for alkane metathesis reported to date.

(ⁱPr⁴PCOP)Ir(C₂H₄) (**3e**)⁴¹ was also found to give a higher turnover number, after 1 h, than the (^tBu⁴PCOP)Ir precursor **3c**, but not as great as obtained with **3d**. Moreover, productivity leveled off with **3e** earlier than with catalysts **3a–d**; it seems likely this is due to bimolecular degradation of the sterically very open complex, possibly dimerization or perhaps a reaction with MoF12. In any case, **3e** seems less promising than **3d**.

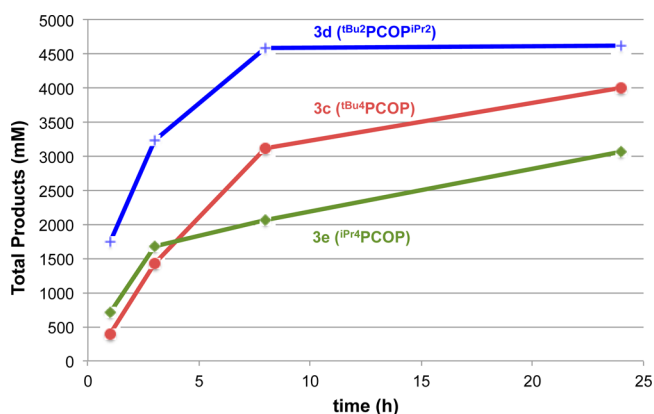
A brief summary of results obtained with all five catalysts is given in Table 5.

Selectivity. The molecular-weight or chain-length selectivity obtained with all three (PCOP)Ir catalysts was similar to that obtained with (^tBu⁴POCOP)Ir and not intermediate between (^tBu⁴POCOP)Ir and (^tBu⁴PCP)Ir (the latter is much more selective for the formation of C_{2n–2} alkanes and ethane from C_n alkanes, in this case *n*-decane and ethane from *n*-hexane). We believe that the large selectivity difference observed for the (^tBu⁴POCOP)Ir and (^tBu⁴PCP)Ir-based catalysts in alkane metathesis reflects a different regioselectivity of alkane dehydrogenation, which results from the two catalysts having a different rate- and product-determining step (e.g., C–H addition, β-H elimination, or olefin extrusion) in the overall alkane dehydrogenation.⁴² The similar selectivity (or lack thereof) in alkane metathesis observed for the (PCOP)Ir complexes and (^tBu⁴POCOP)Ir suggests that these complexes have the same rate- and product-determining step within the alkane dehydrogenation sequence (or at least that they do not share the same rate- and product-determining step as (^tBu⁴PCP)Ir). Further results of selectivity studies will be reported in due course.

Summary. Bisphosphine complex (^tBu⁴PCP)Ir and bisphosphinite complex (^tBu⁴POCOP)Ir, previously reported to catalyze alkane metathesis in tandem with MoF12, catalyze transfer dehydrogenation with similar rates under typical alkane metathesis conditions. Different resting states observed for each catalyst, however, indicate that different segments of the

Table 4. Product Concentrations (mM) of Products Formed by Metathesis of *n*-Hexane (7.5 M) Catalyzed by MoF12 (16 mM) and Catalysts 3d or 3e (10 mM) at 125 °C

Catalyst 3d, (^t Bu ₂ PCOP ⁱ Pr ₂)IrH ₄												
<i>t</i> (h)	C2	C3	C4	C5	C7	C8	C9	<i>trans</i> -5-decene	C10	C11–19	[total product]	selectivity C10/(C7–10)
1	133	339	248	385	224	105	120	4	143	48	1750	0.25
3	220	595	509	754	441	218	204	2	193	99	3234	0.18
8	450	986	764	969	535	278	234	1	190	187	4594	0.15
24	344	974	792	1029	572	293	242	1	189	183	4619	0.15
Catalyst 3e, (ⁱ Pr ₄ PCOP)Ir(C ₂ H ₄)												
<i>t</i> (h)	C2	C3	C4	C5	C7	C8	C9	<i>trans</i> -5-decene	C10	C11–19	[total product]	selectivity C10/(C7–10)
1	25	119	78	179	118	46	69	1	67	10	712	0.23
3	55	307	202	424	256	102	138	3	169	31	1687	0.26
8	70	398	261	521	298	117	153	4	200	44	2066	0.26
24	127	717	463	771	368	146	167	0	197	120	3076	0.22

**Figure 7.** Total alkane products formed in the metathesis of *n*-hexane catalyzed by MoF12 and PCOP catalysts 3c–e.**Table 5.** Summary of Results with All Iridium Catalysts Investigated^a

iridium catalyst	initial TOF (h ⁻¹) ^b	TON ^c (24 h)	selectivity C10/(C7–10)
3a, (^t Bu ₂ PcP ^t Bu ₂)IrH ₂	11	111	0.48
3b, (^t Bu ₂ POCOP ^t Bu ₂)IrH ₂	5.4	134	0.12
3c, (^t Bu ₂ PCOP ^t Bu ₂)IrH ₂	40	400	0.14
3d, (^t Bu ₂ PCOP ⁱ Pr ₂)IrH ₄	175	462	0.15
3e, (ⁱ Pr ₄ PCOP)Ir(C ₂ H ₄)	71	308	0.22

^aConditions as described in text: 16 mM MoF12, 10 mM iridium catalyst in *n*-hexane (7.6 M), TBE (2.0 equiv per mole of catalyst for dihydrides 3a–c, 4.0 equiv per mole for tetrahydride 3d, none for ethene complex 3e). ^bTOF = turnover frequency = moles of product (total alkane products) per mole of iridium catalyst observed after 1 h. ^cTON = turnover frequency = moles of product (total alkanes) per mole of iridium catalyst observed after 24 h.

transfer dehydrogenation cycle are rate-determining in each case. This observation led to the hypothesis that for a species with intermediate properties, neither segment of its catalytic cycle would be as slow as the respective rate-determining segments for (^tBu₄PcP)Ir and (^tBu₄POCOP)Ir, and thus, the overall rate of catalysis would be faster. Indeed, the “hybrid” phosphine–phosphinite catalyst (^tBu₄PCOP)Ir is found to cocatalyze alkane metathesis ~4 and 8 times faster than (^tBu₄PcP)Ir and (^tBu₄POCOP)Ir, respectively, and affords higher total turnover numbers. In accord with the idea that the hybrid catalyst approaches a balance whereby the hydrogenation and dehydrogenation segments of the catalytic

cycle are comparably fast under catalytic conditions, the resting state is found to be a mixture of dihydride and dehydrogenated (olefin-bound) complex.

Decreasing the steric bulk of the phosphine–phosphinite pincer led to the synthesis of catalyst precursor (^tBu₂PCOPⁱPr₂)IrH₄ (3d), which exhibits rates of catalysis about a factor of 4 faster than (^tBu₄PCOP)IrH₂, that is, ~32 times faster than (^tBu₄POCOP)Ir. Further decreasing steric crowding led to a (ⁱPr₄PCOP)Ir precursor (the corresponding ethylene complex) that gave rates faster than (^tBu₄PCOP)Ir but slower than (^tBu₂PCOPⁱPr₂)IrH₄ and appeared to undergo decomposition more readily than the other catalysts studied.

EXPERIMENTAL SECTION

General Information. All manipulations were conducted under an argon atmosphere either in a glovebox or using standard Schlenk techniques. All anhydrous solvents were purchased from Aldrich, flushed with argon, and stored in an argon atmosphere in a glovebox. Mesitylene, *n*-hexane (anhydrous, 99%+), *tert*-butylethylene (TBE; 3,3-dimethyl-1-butene, 97%) were purchased from Aldrich and were distilled over Na/benzophenone and stored in a glovebox. (^tBu₄PcP)IrH₂,³⁵ (^tBu₄POCOP)IrH₂,^{27,34} 3-(bromomethyl)phenol,⁴³ HPⁱPr₂,⁴⁴ and Mo(NAr(CHCMe₂Ph)(OR_{F6})₂) (Ar = 2,6-*i*-PrC₆H₃; OR_{F6} = OMe(CF₃)₂)⁴⁵ were prepared as described previously. ⁱPr₂PcCl and ^tBu₂PcCl were used as purchased from Strem Chemicals, Inc. All other reagents were obtained from commercial sources and used as received. All glassware was placed in a vacuum oven at least 24 h prior to use. Stock solution vials and glass tubes for reaction vessels (5 mm × 120 mm) were flame-dried before being placed in the vacuum oven. NMR spectra were recorded on 400- or 500-MHz Varian VNMRs spectrometers. ¹H NMR spectra are referenced to residual *protio* signal in the deuterated solvent. ³¹P{¹H} NMR chemical shifts are referenced to an external standard consisting of PMe₃ (δ –62.4 ppm) in mesitylene-*d*₁₂ solvent inside a flame-sealed capillary tube. Elemental analyses were performed by Roberston Microlit Laboratories, Ledgewood, New Jersey.

GC Method. Gas chromatography was performed on a Varian 430 gas chromatograph utilizing flame ionization detection with the following parameters:

- Column: 30 m × 0.25 mm × 0.5 μm (Supelco) fused silica capillary column, Petrocol, HD
- Starting temperature: 38 °C
- Time at starting temp: 1.4 min
- Ramp: 20 °C/min to 250 °C, hold time 3 min

Ramp: 280 °C at 30 °C/min, hold time 35 min
 Flow rate: 1 mL/min (He)
 Split ratio: 90
 Ending temp: 280 °C
 Injector temp: 300 °C
 Detector temp: 310 °C

GC Response Factors. The GC response factors for the selected *n*-alkanes (C6, C8, C10, C12, and C15) were obtained experimentally. A known concentration of the alkane and a mesitylene standard was prepared and injected into the GC. The response factor of each alkane was calculated as an average of three independent runs. A plot of response factor versus alkane carbon number was generated and found to be essentially linear; the response factors for alkanes not directly measured were extrapolated from this plot. The R_f of *trans*-5-decene was measured independently.

General Procedure for Alkane Metathesis Catalysis. In an argon-filled glovebox, a 20-mL vial was charged with the (pincer)Ir catalysts (**3a–e**, 0.050 mmol) and the MoF12 catalyst (0.080 mmol). A 5.0 mL portion of an *n*-hexane solution containing mesitylene (0.162 mmol as an internal standard) and TBE (0.100 mmol for dihydrides **3a–c**, 0.200 mmol for tetrahydride **3d**, none for ethene complex **3e**) was added, and the solution was thoroughly mixed. Twelve aliquots of this stock solution (0.400 mL each) were then syringed into glass tubes (5 mm × 120 mm). Vacuum adapters were fixed onto the tubes via plastic tubing to allow for flame-sealing. Samples were frozen in liquid nitrogen, and the headspace was evacuated on a high vacuum line, after which the glass tubes were flame-sealed so that the ratio between liquid phase and headspace was approximately 1:1. The samples were placed in a temperature-calibrated GC oven at 125 °C. Tubes were taken from the oven at appropriate intervals and frozen in liquid nitrogen to minimize the escape of volatile alkanes. The seal of each tube was then broken and quickly capped with a 5-mm rubber septum. The sample was then brought back to room temperature and promptly analyzed by GC.

Resting State of (^{tBu}PCOP)Ir in Alkane Metathesis. A solution of 10 mM ^{tBu}PCOPIr(H)₂ (**3c**, 0.005 mmol), 16 mM MoF12 catalyst (0.008 mmol), 40 mM TBE (0.020 mmol), and roughly 7.6 M *n*-hexane (total volume of solution: 0.5 mL) was added to an NMR tube along with an external PMe₃ in *p*-xylene-*d*₁₀ capillary insert, and the NMR tube was subsequently flame-sealed. This mixture was heated to 90 °C in the NMR spectrometer for ~60 min. After 60 min, ³¹P NMR exhibited two main sets of peaks of differing intensity: a smaller set of peaks indicative of the dihydride species (**3c**, 24%) and larger set of peaks consisting of a doublet at 171.2 ppm and a doublet at 61.6 ppm (76%) indicative of an olefin-bound complex. To confirm the identity of this putative olefin-bound species, in a separate NMR tube, 10 mM ^{tBu}PCOPIrH₂ and 40 mM 1-hexene (in *p*-xylene-*d*₁₀ solution, 0.5 mL total sample volume) were mixed, reproducing the sets of doublets at 171.2 and 61.6 ppm in the ³¹P NMR and confirming that the larger set of peaks is attributable to an olefin-bound species.

Synthesis of 3-(Alkylphosphinomethyl)phenol. A mixture of 3-(bromomethyl)phenol (4.003 g, 21.40 mmol) and HPR₂ (R = ^tPr, 2.554 g, 21.61 mmol; R = ^tBu, 3.161 g, 21.62 mmol) in degassed acetone (30 mL) was heated to reflux for 12 h and then stirred at room temperature overnight. The mother liquor was decanted from the waxy white precipitate that formed, and the precipitate was dried under vacuum. The

precipitate was treated with a saturated solution of aqueous NaHCO₃ (40 mL) and stirred at 80 °C for 6 h. After cooling to room temperature, the mother liquor was cannulated out, and the white precipitate was dried under vacuum. Product was extracted with Et₂O or THF (30 mL × 3) and the combined solution was evaporated under vacuum to obtain the waxy orange products.

3-(*iso*-Propylphosphinomethyl)phenol. Yield: 3.120 g, 13.91 mmol, 65%. (NMR δ, CDCl₃) ¹H: 7.11 (t, $J_{\text{HH}} = 7.75$ Hz, 1H, Ar–H), 6.82 (d, $J_{\text{HH}} = 7.5$ Hz, 1H, Ar–H), 6.77 (s, 1H, Ar–H), 6.63 (d, $J_{\text{HH}} = 9.0$ Hz, 1H, Ar–H), 4.73 (s, 1H, OH), 2.74 (d, $^2J_{\text{PH}} = 1.5$ Hz, 2H, CH₂), 1.74 (d of septet, $^3J_{\text{HH}} = 7.0$ Hz, $^2J_{\text{PH}} = 2.5$ Hz, 2H, CH(CH₃)₂), 1.03–1.09 (m, 12H, CH(CH₃)₂). ¹³C{¹H}: 155.5 (s, Ar–C), 141.9 (d, $J_{\text{PC}} = 8.2$ Hz, Ar–C), 129.5 (s, Ar–C), 121.8 (d, $J_{\text{PC}} = 6.5$ Hz, Ar–C), 116.1 (d, $J_{\text{PC}} = 7.4$ Hz, Ar–C), 112.5 (d, $J_{\text{PC}} = 2.0$ Hz, Ar–C), 29.5 (d, $^1J_{\text{PC}} = 20.1$ Hz, CH₂), 23.3 (d, $^1J_{\text{PC}} = 14.1$ Hz, 2C, CH(CH₃)₂), 19.6 (d, $^2J_{\text{PC}} = 13.4$ Hz, 2C, C(CH₃)₂), 19.2 (d, $^2J_{\text{PC}} = 10.7$ Hz, 2C, CH(CH₃)₂). ³¹P{¹H}: 12.1 (s).

3-(*tert*-Butylphosphinomethyl)phenol. Yield: 4.807 g, 19.05 mmol, 89%. (NMR δ, CDCl₃) ¹H: 7.01 (t, $J_{\text{HH}} = 7.8$ Hz, 1H, Ar–H), 6.82 (d, $J_{\text{HH}} = 7.5$ Hz, 1H, Ar–H), 6.75 (s, 1H, Ar–H), 6.47 (d, $J_{\text{HH}} = 8.0$ Hz, 1H, Ar–H), 4.66 (s, 1H, OH), 2.71 (d, $^2J_{\text{PH}} = 3.5$ Hz, 2H, CH₂), 1.06 (d, $^3J_{\text{PH}} = 11.0$ Hz, 18H, 2 C(CH₃)₃). ¹³C{¹H}: 155.8 (s, Ar–C), 143.8 (d, $J_{\text{PC}} = 12.4$ Hz, Ar–C), 129.7 (s, Ar–C), 122.3 (d, $J_{\text{PC}} = 8.0$ Hz, Ar–C), 116.7 (d, $J_{\text{PC}} = 9.2$ Hz, Ar–C), 112.7 (d, $J_{\text{PC}} = 2.1$ Hz, Ar–C), 32.1 (d, $^1J_{\text{PC}} = 21.7$ Hz, CH₂), 30.1 (d, $^2J_{\text{PC}} = 13.1$ Hz, 6C, C(CH₃)₃), 28.6 (d, $^1J_{\text{PC}} = 23.2$ Hz, 2C, C(CH₃)₃). ³¹P{¹H}: 33.2 (s).

General Procedure for Syntheses of PCOP-H Ligands.

A solution of the appropriate 3-(dialkylphosphinomethyl)phenol (for compound **1c**, R = ^tBu, 2.657 g, 10.53 mmol; for compound **1e**, R = ^tPr, 0.480 g, 2.14 mmol; for compound **1d**, R = ^tBu, 0.540 g, 2.14 mmol) in THF (10 mL; 40 mL in the case of **1c**) was added dropwise to the suspension of NaH (0.2779 g, 11.58 mmol in the case of **1c**; 0.057 g, 2.37 mmol for **1d** and **1e**) in THF (20 mL), and the reaction mixture was heated to reflux for 1.5 h. After cooling to room temperature, the solution of dialkylchlorophosphine, R'₂P-Cl (for compound **1c**, R' = ^tBu, 2.00 mL, 10.50 mmol; for compound **1e** and **1d**, R' = ^tPr, 0.326 g, 2.14 mmol) in THF (10 mL) was added dropwise through a cannula, and the resultant reaction mixture was heated to reflux for 2 h. The solvent was then removed under vacuum, and the product was extracted with pentane (20 mL × 2). The combined pentane solution was removed under vacuum to obtain a pale yellow viscous liquid product.

^{tBu}PCOP-H (**1c**). Yield: 3.514 g, 8.862 mmol, 84%. (NMR, δ, C₆D₆) ¹H: 7.62 (s, 1H, Ar–H_{ipso}), 7.10–7.18 (m, 3 H, Ar–H), 2.80 (d, $^2J_{\text{PH}} = 2.25$ Hz, 2H, CH₂), 1.21 (d, $^3J_{\text{PH}} = 11.6$ Hz, 18 H, C(CH₃)₃), 1.11 (d, $^3J_{\text{PH}} = 10.5$ Hz, 18H, C(CH₃)₃). ¹³C{¹H}: 160.3 (d, $^3J_{\text{PC}} = 9.4$ Hz, Ar–C_{ipso}), 143.7 (dd, $J_{\text{PC}} = 12.7$ Hz, $J_{\text{PC}} = 0.7$ Hz, Ar–C), 129.5 (s, Ar–C), 123.3 (dd, $J_{\text{PC}} = 8.7$ Hz, $J_{\text{PC}} = 1.2$ Hz, Ar–C), 120.1 (dd, $J_{\text{PC}} = 11.3$ Hz, $J_{\text{PC}} = 9.1$ Hz, Ar–C), 115.9 (dd, $J_{\text{PC}} = 10.5$ Hz, $J_{\text{PC}} = 1.9$ Hz, Ar–C), 35.7 (d, $^1J_{\text{PC}} = 26.8$ Hz, CH₂), 31.8 (d, $^1J_{\text{PC}} = 24.5$, C(CH₃)₃), 30.0 (d, $^2J_{\text{PC}} = 13.5$ Hz, C(CH₃)₃), 29.2 (d, $^1J_{\text{PC}} = 25.8$ Hz, C(CH₃)₃), 27.6 (d, $^2J_{\text{PC}} = 15.8$ Hz, C(CH₃)₃). ³¹P{¹H}: 152.7 (s, O–P), 34.1 (s, CH₂–P).

^{tBu}PCOP^{Pr}2-H (**1d**). Yield: 0.591 g, 1.604 mmol, 75%. (NMR, δ, C₆D₆) ¹H: 7.47 (s, 1H, Ar–H_{ipso}), 7.08 (d, $J_{\text{HH}} = 4.0$ Hz, 2H, Ar–H), 7.03 (t, $J_{\text{HH}} = 4.0$ Hz, 1H, Ar–H), 2.71 (d, $^2J_{\text{PH}} = 2.0$ Hz, 2H, CH₂), 1.77 (d of septet, $^3J_{\text{HH}} = 5.0$ Hz, $^2J_{\text{PH}} = 2.5$ Hz,

2H, CH(CH₃)₂), 1.15 (dd, ³J_{HH} = 10.3 Hz, ³J_{PH} = 6.6 Hz, 6H, 2CH(CH₃), 1.03 (d, ³J_{PH} = 10.6 Hz, 18H, C(CH₃)₃), 0.99 (dd, ³J_{HH} = 10.2 Hz, ³J_{PH} = 7.4 Hz, 6H, 2CH(CH₃)). ¹³C{¹H}: 160.4 (d, J_{PC} = 9.0 Hz, Ar-C), 144.3 (d, J_{PC} = 12.4 Hz, Ar-C), 137.6 (s, Ar-C), 124.0 (dd, J_{PC} = 9.0 Hz, J_{PC} = 1.1 Hz, Ar-C), 120.9 (dd, J_{PC} = 10.7 Hz, J_{PC} = 9.4 Hz), 116.6 (dd, J_{PC} = 10.5 Hz, J_{PC} = 1.9 Hz, Ar-C), 32.3 (d, ¹J_{PC} = 24.4 Hz, CH₂), 30.5 (d, ²J_{PC} = 13.4 Hz, C(CH₃)₃), 29.6 (d, ¹J_{PC} = 25.8 Hz, C(CH₃)₃), 29.2 (d, ¹J_{PC} = 18.6 Hz, CH(CH₃)₃), 18.5 (d, ²J_{PC} = 20.5 Hz, C(CH₃)₂), 17.8 (d, ²J_{PC} = 8.6 Hz, C(CH₃)₂). ³¹P{¹H}: 147.1 (s, O-P), 33.5 (s, CH₂-P).

^{iPr}PCOP-H (**1e**). Yield: 0.561 g, 1.65 mmol, 77%. (NMR, δ, C₆D₆) ¹H: 7.43 (br s, 1H, Ar-H_{ipso}), 7.12–7.07 (m, 2H, Ar-H), 6.96 (d, J_{HH} = 7.0 Hz, 1H, Ar-H), 2.64 (s, 2H, CH₂), 1.78 (d of septet, ³J_{HH} = 7.0 Hz, ²J_{PH} = 2.5 Hz, 2H, OPCH(CH₃)₂), 1.57 (d of septet, ³J_{HH} = 7.0 Hz, ²J_{PH} = 2.0 Hz, 2H, PCH(CH₃)₂), 1.16 (dd, ³J_{HH} = 10.5 Hz, ³J_{PH} = 7.0 Hz, 6H, CH(CH₃), 1.02–0.99 (m, 18H, CH(CH₃)₂). ¹³C{¹H}: 160.4 (d, ⁴J_{PC} = 8.5 Hz, Ar-C_{ipso}), 142.5 (d, J_{PC} = 8.23 Hz, Ar-C), 129.6 (s, Ar-C), 123.2 (dd, J_{PC} = 5.8 Hz, J_{PC} = 1.1 Hz, Ar-C), 120.0 (dd, J_{PC} = 10.8 Hz, J_{PC} = 7.4 Hz), 116.2 (dd, J_{PC} = 10.5 Hz, J_{PC} = 2.0 Hz, Ar-C), 30.2 (d, ¹J_{PC} = 22.2 Hz, CH₂), 28.6 (d, ¹J_{PC} = 18.5 Hz, 2C, CH(CH₃)₂), 23.8 (d, ¹J_{PC} = 16.2 Hz, 2C, CH(CH₃)₂), 19.8 (d, ²J_{PC} = 14.4 Hz, CH(CH₃)₂), 19.3 (d, ²J_{PC} = 11.2 Hz, CH(CH₃)₂), 17.9 (d, ²J_{PC} = 20.6 Hz, CH(CH₃)₂), 17.2 (d, ²J_{PC} = 8.7 Hz, CH(CH₃)₂). ³¹P{¹H}: 147.4 (s, O-P), 10.2 (s, CH₂-P).

General Procedure for Syntheses of (PCOP)IrHCl Complexes. A mixture of the appropriate (^RPCOP^R-H) (3.0 mL of 0.367 M solution in toluene for **1c**, 1.1 mmol; 0.462 g of **1e**, 1.36 mmol; 0.500 g of **1d**, 1.36 mmol) and [Ir(COD)Cl]₂ (0.335 g, 0.499 mmol for **1c**; 0.434 g, 0.646 mmol for **1e** and **1d**) in toluene (15 mL) was heated to reflux (72 h for **1c**, 3 h for **1e**, and 12 h for **1d**) under H₂ atmosphere. After cooling the reaction mixture to room temperature, the mother liquor was evaporated under vacuum. The product was extracted with pentane (60 mL × 3) and the combined pentane solution was evaporated to obtain the orange-red crystalline products of **2c–e**.

^{tBu}PCOP)IrHCl (**2c**). Yield: 0.470 g, 0.753 mmol, 68%. (NMR, δ, C₆D₆) ¹H: 6.93–6.83 (m, 3H, Ar-H), 3.10 (dd, ²J_{HH} = 17.6 Hz, ²J_{PH} = 9.5 Hz, 1H, CH₂), 3.00 (dd, ²J_{HH} = 17.6 Hz, ²J_{PH} = 8.9 Hz, 1H, CH₂), 1.34 (d, ³J_{PH} = 14.0 Hz, 9H, C(CH₃)₃), 1.29 (d, ³J_{PH} = 14.2 Hz, 9H, C(CH₃)₃), 1.22 (d, ³J_{PH} = 13.0 Hz, 9H, C(CH₃)₃), 1.19 (d, ³J_{PH} = 13.4 Hz, 9H, C(CH₃)₃), -41.38 (dd, ²J_{PH} = 13.3 Hz, ²J_{PH} = 12.3 Hz). ¹³C{¹H}: 168.1 (apparent t, ³J_{PC} = 6.1 Hz, Ar-C_{ipso}), 152.0 (dd, J_{PC} = 11.3 Hz, J_{PC} = 5.5 Hz, Ar-C), 132.2 (dd, J_{PC} = 5.6 Hz, J_{PC} = 3.0 Hz, Ar-C), 124.6 (s, Ar-C), 118.1 (d, J_{PC} = 15.5 Hz, Ar-C), 108.5 (d, J_{PC} = 11.7 Hz, Ar-C), 43.6 (dd, ¹J_{PC} = 19.3 Hz, ³J_{PC} = 4.9 Hz, C(CH₃)₃), 39.4 (dd, ¹J_{PC} = 20.9 Hz, ³J_{PC} = 5.9 Hz, C(CH₃)₃), 37.5 (dd, ¹J_{PC} = 15.9 Hz, ³J_{PC} = 3.2 Hz, C(CH₃)₃), 35.3 (dd, ¹J_{PC} = 29.8 Hz, ³J_{PC} = 1.0 Hz, CH₂), 35.0 (dd, ¹J_{PC} = 17.7 Hz, ³J_{PC} = 3.3 Hz, C(CH₃)₃), 29.9 (dd, ²J_{PC} = 3.8 Hz, ⁴J_{PC} = 1.3 Hz, C(CH₃)₃), 29.3 (dd, ²J_{PC} = 3.8 Hz, ⁴J_{PC} = 1.3 Hz, C(CH₃)₃), 27.8 (d, ²J_{PC} = 4.9 Hz, C(CH₃)₃), 27.7 (dd, ²J_{PC} = 4.9 Hz, ⁴J_{PC} = 1.0 Hz, C(CH₃)₃). ³¹P{¹H}: 168.6 (dd, ²J_{PP} = 345.0 Hz, ²J_{PH} = 12.3 Hz, O-P), 70.6 (dd, ²J_{PP} = 345.0 Hz, ²J_{PH} = 11.0 Hz, CH₂-P). Anal. Calcd. for C₂₃H₄₂OIrP₂Cl: C, 44.26; H, 6.78; Cl, 5.68. Found: C, 44.03; H, 6.59; Cl, 5.67.

^{tBu}PCOP^{iPr}2)IrHCl (**2d**). Yield: 0.662 g, 1.11 mmol, 86%. (NMR, δ, C₆D₆) ¹H: 6.84–6.89 (m, 3H, Ar-H), 3.10 (apparent septet, ²J_{HaHb} = 18.3 Hz, ²J_{HP} = 9.0 Hz, CH_aH_b), 2.69 (septet, ³J_{HH} = 7.0 Hz, 1H, CH(CH₃)₂), 2.28 (septet, ³J_{HH} = 6.0 Hz, 1H, CH(CH₃)₂), 1.27 (dd partially obscured by another signal, J_{HH} = 7.2 Hz, CH(CH₃)₂), 1.21 (dd, J_{HH} = 13.1 Hz, 18H, C(CH₃)₃), 1.16 (dd partially obscured by another signal, J_{HH} = 6.5 Hz, CH(CH₃)₂), 1.12 (dd partially obscured by another signal, J_{HH} = 6.0 Hz, CH(CH₃)₂), 0.99 (dd, J_{HH} = 7.0 Hz, CH(CH₃)₂), -39.45 (dd, ²J_{PH} = 15.7 Hz, ²J_{PH} = 11.0 Hz). ¹³C{¹H}: 137.0 (s, Ar-C), 127.3 (d, J_{PC} = 18.2 Hz, Ar-C), 126.7 (d, J_{PC} = 23.4 Hz, Ar-C), 124.4 (s, Ar-C), 118.3 (d, J_{PC} = 15.3 Hz, Ar-C), 108.6 (d, J_{PC} = 12.1 Hz, Ar-C), 38.3 (dd, J_{PC} = 16.0 Hz, J_{PC} = 3.3 Hz, CH(CH₃)₂), 35.1 (dd, J_{PC} = 17.3 Hz, J_{PC} = 3.3 Hz, CH(CH₃)₂), 34.9 (d, ¹J_{PC} = 30.4 Hz, CH₂), 30.6 (dd, J_{PC} = 25.7 Hz, J_{PC} = 4.3 Hz, C(CH₃)₃), 29.1 (dd, J_{PC} = 29.8 Hz, J_{PC} = 5.1 Hz, C(CH₃)₃), 17.4 (br s, C(CH₃)₃), 16.8 (d, J_{PC} = 7.4 Hz, CH(CH₃)₂), 16.7 (dd, J_{PC} = 3.3 Hz, J_{PC} = 1.9 Hz, C(CH₃)₂), 16.6 (d, ¹J_{PC} = 11.9 Hz, C(CH₃)₃), 16.4 (d, ¹J_{PC} = 13.3 Hz, CH(CH₃)₃). ³¹P{¹H}: 165.4 (dd, ²J_{PP} = 350 Hz, ²J_{PH} = 12.0 Hz, O-P), 72.9 (dd, ²J_{PP} = 350 Hz, ²J_{PH} = 8.0 Hz, CH₂-P). Anal. Calcd. for C₁₉H₃₄OIrP₂Cl: C, 42.31; H, 6.24; Cl, 5.95. Found: C, 42.59; H, 6.37; Cl, 5.81.

^{iPr}PCOP)IrHCl (**2e**). Yield: 0.462 g, 0.814 mmol, 63%. (NMR, δ, C₆D₆) ¹H: 6.89–6.85 (m, 2H, Ar-H), 6.78 (d, J_{HH} = 2.0 Hz, 1H, Ar-H), 2.75 (apparent qd, ²J_{HaHb} = 18.0 Hz, ²J_{PH} = 9.3 Hz, 2H, CH_aH_b), 2.65–2.69 (m, 1H, CH(CH₃)₂), 2.27 (d of septet, ³J_{HH} = 4.5 Hz, ²J_{PH} = 2.5 Hz, 1H, CH(CH₃)₂), 2.05–2.08 (m, 1H, CH(CH₃)₂), 1.95 (d of septet, ³J_{HH} = 6.5 Hz, ²J_{PH} = 1.5 Hz, 1H, CH(CH₃)₂), 1.29 (dd partially obscured by another signal, ³J_{HH} = 17.0 Hz, ³J_{PH} = 7.0 Hz, 3H, CH(CH₃)₂), 1.17 (dd, ³J_{HH} = 17.0 Hz, ³J_{PH} = 7.5 Hz, 3H, CH(CH₃)₂), 1.16–1.13 (m, 6H, CH(CH₃)₂), 1.11 (dd partially obscured by another signal, ³J_{HH} = 11.0 Hz, ³J_{PH} = 7.5 Hz, 3H, CH(CH₃)₂), 1.03 (dd, ³J_{HH} = 15.5 Hz, ³J_{PH} = 7.0 Hz, 3H, CH(CH₃)₂), 0.87–0.82 (m, 6H, CH(CH₃)₂), -36.54 (apparent t, ²J_{PH} = 13.8 Hz). ¹³C{¹H}: 166.3 (s, Ar-C_{ipso}), 149.7 (s, Ar-C), 124.2 (s, Ar-C), 118.5 (d, ²J_{PC} = 16.3 Hz, Ar-C), 109.2 (d, ²J_{PC} = 11.7 Hz, Ar-C), 33.3 (d, ¹J_{PC} = 32.0 Hz, CH₂), 31.3 (dd, ¹J_{PC} = 25.4 Hz, ³J_{PC} = 5.0 Hz, CH(CH₃)₂), 29.3 (dd, ¹J_{PC} = 29.0 Hz, ³J_{PC} = 5.1 Hz, CH(CH₃)₂), 25.1 (dd, ²J_{PC} = 23.6 Hz, ⁴J_{PC} = 2.4 Hz, CH(CH₃)₂), 24.6 (dd, ²J_{PC} = 25.9 Hz, ⁴J_{PC} = 2.6 Hz, CH(CH₃)₂), 18.3 (dd, ²J_{PC} = 12.4 Hz, ⁴J_{PC} = 4.0 Hz, 4C, CH(CH₃)₂), 17.1 (dd, ²J_{PC} = 11.0 Hz, ⁴J_{PC} = 3.8 Hz, 4C, CH(CH₃)₂). ³¹P{¹H}: 168.2 (dd, ²J_{PP} = 355 Hz, J_{PH} = 8.5 Hz, O-P), 60.7 (dd, J_{PP} = 356 Hz, J_{PH} = 3.2 Hz, CH₂-P). Unknown species (12% based upon integrals from ¹H NMR), (NMR, δ, C₆D₆): ¹H -25.2, (J_{HH} = 17.0 Hz, J_{PH} = 11.0 Hz), ³¹P{¹H}: 150.5 (dd, ²J_{PP} = 361 Hz, ²J_{PH} = 8.1 Hz), 42.0 (dd, ²J_{PP} = 363 Hz, ²J_{PH} = 5.4 Hz). Anal. Calcd. for C₁₉H₃₄OIrP₂Cl: C, 40.17; H, 6.03; Cl, 6.24. Found: C, 42.15; H, 6.17; Cl, 6.40.⁴⁷

General Procedure for Syntheses of (PCOP)Ir(L). The (PCOP)IrHCl (0.150 g, 0.247 mmol of **2c**; 0.200 g, 0.352 mmol of **2e**; 0.210 g, 0.352 mmol of **2d**) was dissolved in pentane (60 mL), and a 1.0 M solution (in THF) of LiBEt₃H (0.25 mL, 0.25 mmol for **2c**; 0.35 mL, 0.35 mmol for **2e** and **2d**) was added dropwise via syringe under hydrogen or ethylene atmosphere, causing the orange solution to turn a pale yellow (brownish in the case of **2e**) and resulting in the precipitation of a white solid. The reaction mixture was stirred for 30 min prior to cannula filtration of the solution. The

pentane solution was evaporated under vacuum to obtain a red crystalline solid of **3c**, orange solid of **3d**, and brownish solid of **3e**. In the case of complex **3d**, the product was obtained as a mixture of (^tBu₂PCOP^{ipr2})IrH₄ and (^tBu₂PCOP^{ipr2})IrH₂ in an 85:15 ratio based upon ¹H NMR spectroscopy. The calculated yield is based on (^tBu₂PCOP^{ipr2})IrH₄.

(^tBu₄PCOP)IrH₂ (**3c**). Yield: 0.136 g, 0.231 mmol, 93%. (NMR, δ, C₆D₆) ¹H: 7.23–7.13 (m, 3H, Ar–H), 3.50 (d, ²J_{PH} = 8.4 Hz, 2H, CH₂), 1.34 (d, ³J_{PH} = 13.8 Hz, 18H, C(CH₃)₃), 1.19 (d, ³J_{PH} = 12.9 Hz, 18H, C(CH₃)₃), –18.12 (apparent t, ²J_{PH} = 8.6 Hz, 2H, IrH₂). ¹³C{¹H}: 171.0 (dd, ³J_{PC} = 5.7 Hz, ³J_{PC} = 3.1 Hz, Ar–C_{ipso}), 170.7 (dd, J_{PC} = 8.5 Hz, J_{PC} = 7.0 Hz, Ar–C), 157.6 (dd, J_{PC} = 14.2 Hz, J_{PC} = 5.8 Hz, Ar–C), 129.5 (dd, J_{PC} = 0.6 Hz, Ar–C), 116.3 (d, J_{PC} = 16.1 Hz, Ar–C), 107.7 (d, J_{PC} = 12.5 Hz, Ar–C), 40.3 (d, ¹J_{PC} = 28.6 Hz, CH₂), 40.1 (dd, ¹J_{PC} = 20.7 Hz, ³J_{PC} = 4.6 Hz, C(CH₃)₃), 35.1 (dd, ¹J_{PC} = 17.6 Hz, ³J_{PC} = 2.4 Hz, C(CH₃)₃), 29.9 (dd, ²J_{PC} = 5.3 Hz, ⁴J_{PC} = 0.8 Hz, C(CH₃)₃), 29.0 (d, ²J_{PC} = 6.3 Hz, C(CH₃)₃). ³¹P{¹H}: 200.3 (d, ²J_{PP} = 330 Hz, O–P), 87.3 (d, ²J_{PP} = 330 Hz, CH₂–P). Anal. Calcd. for C₂₃H₄₃OIrP₂: C, 46.84; H, 7.35. Found: C, 41.89; H, 6.55.⁴⁷

(^tBu₂PCOP^{ipr2})IrH₄ (**3d**). Yield: 0.185 g, 0.329 mmol, 94%. (NMR, δ, *p*-Xyl-*d*₁₀) ¹H: 6.91 (t, J_{PH} = 7.5 Hz, 1H, Ar–H), 6.82 (d, J_{PH} = 7.4 Hz, 1H, Ar–H), 6.79 (d, J_{PH} = 7.8 Hz, 1H, Ar–H), 3.23 (d, J_{PH} = 9.0 Hz, 2H, CH₂), 2.19 (septet, ³J_{HH} = 2.2 Hz, 2H, CH(CH₃)₂), 1.16 (d, ³J_{PH} = 12.8 Hz, 18H, C(CH₃)₃), 1.07 (dd, ³J_{HH} = 15.0 Hz, ³J_{PH} = 7.0 Hz, 6H, 2CH(CH₃)), 0.98 (dd, ³J_{HH} = 17.7 Hz, ³J_{PH} = 7.0 Hz, 6H, 2CH(CH₃)), –8.74 (t, ²J_{PH} = 9.7 Hz, 4H, Ir–H). ¹³C{¹H}: 163.4 (apparent t, J_{PC} = 9.5 Hz, Ar–C), 148.5 (Ar–C), 135.1 (br s, Ar–C), 124.7 (s, Ar–C), 117.2 (apparent t, J_{PC} = 23.7 Hz, Ar–C), 107.6 (apparent t, J_{PC} = 19.6 Hz, Ar–C), 40.7 (d, ¹J_{PC} = 31.8 Hz, CH₂), 32.5 (d, ¹J_{PC} = 18.5 Hz, C(CH₃)₂), 30.4 (d, ²J_{PC} = 3.5 Hz, C(CH₃)₂), 18.5 (d, ²J_{PC} = 10.5 Hz, HC(CH₃)₂), 17.9 (br s, C(CH₃)₂). ³¹P{¹H}: 171.2 (d, ²J_{PP} = 327 Hz, O–P), 69.8 (d, ²J_{PP} = 327 Hz, CH₂–P). (^tBu₂PCOP^{ipr2})IrH₂ ¹H: –17.2 (br s 2H, Ir–H). ³¹P{¹H}: 188.9 (d, ²J_{PP} = 331, O–P), 87.2 (d, ²J_{PP} = 330 Hz, CH₂–P). Anal. Calcd. for C₂₁H₄₁OIrP₂: C, 44.74; H, 7.33. Found: C, 41.83; H, 6.35.⁴⁷

(^{ipr4}PCOP)Ir(C₂H₄) (**3e**). Yield: 0.187 g, 0.334 mmol, 95%. (NMR, δ, *p*-Xyl-*d*₁₀) ¹H: 7.09 (d, ³J_{HH} = 7.5 Hz, 1H, Ar–H), 7.02–6.90 (m, 2H, Ar–H), 2.98 (d, ²J_{PH} = 9.5 Hz, 2H, CH₂), 2.67 (apparent t, ²J_{HH} = 2.5 Hz, 4H, C₂H₄), 2.35 (d of septet, ³J_{HH} = 7.0 Hz, ²J_{PH} = 2.0 Hz, 2H, CH(CH₃)₂), 2.09 (d of septet, ³J_{HH} = 7.0 Hz, ²J_{PH} = 2.0 Hz, 2H, CH(CH₃)₂), 1.18 (dd, ³J_{HH} = 11.5 Hz, ³J_{PH} = 7.0 Hz, 6H, CH(CH₃)₂), 1.10 (dd, ³J_{HH} = 16.0 Hz, ³J_{PH} = 7.0 Hz, 6H, CH(CH₃)₂), 1.03 (dd, ³J_{HH} = 15.5 Hz, ³J_{PH} = 7.0 Hz, 6H, CH(CH₃)₂), 0.92 (dd, ³J_{HH} = 12.5 Hz, ³J_{PH} = 7.0 Hz, 6H, CH(CH₃)₂). ¹³C{¹H}: 165.9 (dd, ³J_{PC} = 12.8 Hz, ³J_{PC} = 7.8 Hz, Ar–C_{ipso}), 157.8 (dd, J_{PC} = 8.5 Hz, J_{PC} = 6.3 Hz, Ar–C), 149.3 (dd, J_{PC} = 17.7 Hz, J_{PC} = 5.3 Hz, Ar–C), 123.9 (s, Ar–C), 116.3 (d, J_{PC} = 18.0 Hz, Ar–C), 107.0 (d, J_{PC} = 14.3 Hz, Ar–C), 37.3 (d, ¹J_{PC} = 31.5 Hz, 1C, CH₂), 34.1 (apparent t, ²J_{PC} = 1.5 Hz, 2C, C₂H₄), 29.8 (dd, ¹J_{PC} = 29.4 Hz, ³J_{PC} = 3.7 Hz, 2C, CH(CH₃)₂), 25.2 (dd, ¹J_{PC} = 25.4 Hz, ³J_{PC} = 1.5 Hz, 2C, CH(CH₃)₂), 17.8 (d, ²J_{PC} = 4.2 Hz, 2C, CH(CH₃)₂), 17.5 (br s, 2C, CH(CH₃)₂), 17.1 (d, ²J_{PC} = 5.3 Hz, 2C, CH(CH₃)₂), 16.6 (br s, 2C, CH(CH₃)₂). ³¹P{¹H}: 175.0 (d, ²J_{PP} = 286 Hz, O–P), 55.6 (d, ²J_{PP} = 286 Hz, CH₂–P). Anal. Calcd. for C₂₁H₃₇OIrP₂: C, 45.07; H, 6.66. Found: C, 43.76; H, 6.35.⁴⁷

■ ASSOCIATED CONTENT

Supporting Information

Crystal structure data of complexes **2c** and **2d**, NMR spectra of complexes **3c** and **3d**, and ³¹P NMR spectrum of (^tBu₄PCOP)Ir during alkane metathesis illustrating the catalyst resting state. This material is available free of charge via the Internet at <http://pubs.acs.org>.

■ AUTHOR INFORMATION

Corresponding Author

*E-mail: alan.goldman@rutgers.edu.

Present Address

¹(C.S.) Department of Chemistry & Biochemistry, Rowan University, Glassboro, NJ 08028, United States

Notes

The authors declare no competing financial interest.

■ ACKNOWLEDGMENTS

This work was supported by NSF through the CCI Center for Enabling New Technologies through Catalysis (CENTC), CHE-1205189 and CHE-0650456. J.D.H. is supported by an NSF-IGERT fellowship (NSF DGE 0903675).

■ REFERENCES

- (1) Brandt, A. R.; Millard-Ball, A.; Ganser, M.; Gorelick, S. M. *Environ. Sci. Technol.* **2013**, *47*, 8031.
- (2) Kerr, R. A. *Science* **2011**, *331*, 1510–1511.
- (3) Murray, J.; King, D. *Nature* **2012**, *481*, 433–435.
- (4) International Energy Agency (IAE) World Energy Outlook 2010; http://www.worldenergyoutlook.org/docs/weo2010/WEO2010_english.pdf
- (5) (a) Dry, M. E. *J. Chem. Technol. Biotechnol.* **2001**, *77*, 43–50. (b) Dry, M. E. *Catal. Today* **2002**, *71*, 227–241. (c) Dry, M. E. *Appl. Catal., A* **2004**, *276*, 1–3.
- (6) Leckel, D. *Energy Fuels* **2009**, *23*, 2342–2358.
- (7) Holdebrandt, D.; Glasser, D.; Hausberger, B.; Patel, B.; Glasser, B. J. *Science* **2009**, *323*, 1680–1681.
- (8) Zwart, R.; van Ree, R. *Biofuels* **2009**, *95*–116.
- (9) Digman, B.; Joo, H. S.; Kim, D.-S. *Environ. Prog.* **2009**, *28*, 47–51.
- (10) Demirbas, A. *Prog. Energy Combust.* **2007**, *33*, 1–18.
- (11) Huber, G. W.; Iborra, S.; Corma, A. *Chem. Rev.* **2006**, *106*, 4044–4098.
- (12) Demirbas, A.; Dincer, K. *Energy Sources, Part A* **2008**, *30*, 1233–1241.
- (13) Centi, G.; Perathoner, S. *Catal. Today* **2009**, *148*, 191–205.
- (14) Wang, W.; Wang, S. P.; Ma, X. B.; Gong, J. L. *Chem. Soc. Rev.* **2011**, *40*, 3703–3727.
- (15) Borodko, Y.; Somorjai, G. A. *Appl. Catal., A* **1999**, *186*, 355–362.
- (16) Graves, C.; Ebbesen, S. D.; Mogensen, M.; Lackner, K. S. *Renew. Sust. Energy Rev.* **2011**, *15*, 1–23.
- (17) *The Outlook for Energy: A View to 2040*, ExxonMobil report, 2012, p 19; http://www.exxonmobil.com/Corporate/files/news_public.pdf.
- (18) Burnett, R. L.; Hughes, T. R. *J. Catal.* **1973**, *31*, 55–64.
- (19) (a) Basset, J. M.; Coperet, C.; Lefort, L.; Maunders, B. M.; Maury, O.; Le Roux, E.; Saggio, G.; Soignier, S.; Soulivong, D.; Sunley, G. J.; Taoufik, M.; Thivolle-Cazat, J. *J. Am. Chem. Soc.* **2005**, *127*, 8604–8605. (b) Soulivong, D.; Coperet, C.; Thivolle-Cazat, J.; Basset, J.-M.; Maunders, B. M.; Pardy, R. B. A.; Sunley, G. J. *Angew. Chem., Int. Ed.* **2004**, *43*, 5366–5369. (c) Vidal, V.; Theolier, A.; Thivolle-Cazat, J.; Basset, J.-M. *Science* **1997**, *276*, 99–102.
- (20) Goldman, A. S.; Roy, A. H.; Huang, Z.; Ahuja, R.; Schinski, W.; Brookhart, M. *Science* **2006**, *312*, 257–261.
- (21) Haibach, M. C.; Kundu, S.; Brookhart, M.; Goldman, A. S. *Acc. Chem. Res.* **2012**, *45*, 947–958.

- (22) Dobereiner, G. E.; Crabtree, R. H. *Chem. Rev.* **2010**, *110*, 681–703.
- (23) Bailey, B. C.; Schrock, R. R.; Kundu, S.; Goldman, A. S.; Huang, Z.; Brookhart, M. *Organometallics* **2009**, *28*, 355–360.
- (24) (a) Huang, Z.; Brookhart, M.; Goldman, A. S.; Kundu, S.; Ray, A.; Scott, S. L.; Vicente, B. C. *Adv. Synth. Catal.* **2009**, *351*, 188–206. (b) Huang, Z.; Rolfe, E.; Carson, E. C.; Brookhart, M.; Goldman, A. S.; El-Khalafy, S. H.; MacArthur, A. H. R. *Adv. Synth. Catal.* **2010**, *352*, 125–135.
- (25) Kundu, S.; Choliy, Y.; Zhuo, G.; Ahuja, R.; Emge, T. J.; Warmuth, R.; Brookhart, M.; Krogh-Jespersen, K.; Goldman, A. S. *Organometallics* **2009**, *28*, 5432–5444.
- (26) Choi, J.; MacArthur, A. H. R.; Brookhart, M.; Goldman, A. S. *Chem. Rev.* **2011**, *111*, 1761–1779.
- (27) (a) Krogh-Jespersen, K.; Czerw, M.; Kanzelberger, M.; Goldman, A. S. *J. Chem. Inf. Comput. Sci.* **2001**, *41*, 56–63. (b) Renkema, K. B.; Kissin, Y. V.; Goldman, A. S. *J. Am. Chem. Soc.* **2003**, *125*, 7770–7771.
- (28) Göttker-Schnetmann, I.; Brookhart, M. *J. Am. Chem. Soc.* **2004**, *126*, 9330–9338.
- (29) Göttker-Schnetmann, I.; White, P. S.; Brookhart, M. *Organometallics* **2004**, *23*, 1766–1776.
- (30) Göttker-Schnetmann, I.; White, P.; Brookhart, M. *J. Am. Chem. Soc.* **2004**, *126*, 1804–1811.
- (31) Kundu, S. K. Ph. D. Thesis, Rutgers University, 2010.
- (32) Renkema, K. B.; Kissin, Y. V.; Goldman, A. S. *J. Am. Chem. Soc.* **2003**, *125*, 7770–7771.
- (33) Eberhard, M. R.; Matsukawa, S.; Yamamoto, Y.; Jensen, C. M. *J. Organomet. Chem.* **2003**, *687*, 185–189.
- (34) Moulton, C. J.; Shaw, B. L. *J. Chem. Soc., Dalton Trans.* **1976**, 1020–1024.
- (35) Gupta, M.; Hagen, C.; Kaska, W. C.; Cramer, R. E.; Jensen, C. M. *J. Am. Chem. Soc.* **1997**, *119*, 840–841.
- (36) Punji, B.; Emge, T. J.; Goldman, A. S. *Organometallics* **2010**, *29*, 2702–2709.
- (37) Huang, Z. Ph. D. thesis, University of North Carolina at Chapel Hill, 2009.
- (38) (a) Schrock, R. R. *Chem. Rev.* **2002**, *102*, 145–179. (b) Schrock, R. R.; Czekelius, C. *Adv. Synth. Catal.* **2007**, *349*, 55–77. (c) Schrock, R. R. *Adv. Synth. Catal.* **2007**, *349*, 41–53.
- (39) Dobereiner, G. E.; Yuan, J.; Schrock, R. R.; Goldman, A. S.; Hackenberg, J. D. *J. Am. Chem. Soc.* **2013**, *135*, 12572–12575.
- (40) Liu, F.; Goldman, A. S. *Chem. Commun.* **1999**, 655–656.
- (41) Ahuja, R.; Punji, B.; Findlater, M.; Supplee, C.; Schinski, W.; Brookhart, M.; Goldman, A. S. *Nat. Chem.* **2011**, *3*, 167–171.
- (42) Biswas, S.; Zhou, T.; Wang, D. Y.; Hackenberg, J.; Nawara-Hultsch, A.; Schrock, R. R.; Brookhart, M.; Krogh-Jespersen, K.; Goldman, A. S. *Abstracts of Papers*, 245th ACS National Meeting & Exposition, New Orleans, LA, April 7–11, 2013, INOR-681.
- (43) Przybilla, K. J.; Vogtle, F. *Chem. Ber.* **1989**, *122*, 347–355.
- (44) Zhu, K.; Achord, P. D.; Zhang, X.; Krogh-Jespersen, K.; Goldman, A. S. *J. Am. Chem. Soc.* **2004**, *126*, 13044–13053.
- (45) Schrock, R. R.; Murdzek, J. S.; Bazan, G. C.; Robbins, J.; DiMare, M.; O'Regan, M. *J. Am. Chem. Soc.* **1990**, *112*, 3875–3886.
- (46) In principle, six aromatic signals should be present in the spectrum, but only five are observed, most likely due to overlap of one peak with the C₆D₆ solvent peak.
- (47) A satisfactory microanalysis was not obtained for this sample.